

# Generic Contrast Agents

Our portfolio is growing to serve you better. Now you have a *choice*.



[VIEW CATALOG](#)

# AJNR

## **Flat Detector CT in the Evaluation of Brain Parenchyma, Intracranial Vasculature, and Cerebral Blood Volume: A Pilot Study in Patients with Acute Symptoms of Cerebral Ischemia**

This information is current as of May 9, 2025.

T. Struffert, Y. Deuerling-Zheng, S. Kloska, T. Engelhorn, C.M. Strother, W.A. Kalender, M. Köhrmann, S. Schwab and A. Doerfler

*AJNR Am J Neuroradiol* 2010, 31 (8) 1462-1469

doi: <https://doi.org/10.3174/ajnr.A2083>

<http://www.ajnr.org/content/31/8/1462>

ORIGINAL  
RESEARCH

T. Struffert  
Y. Deuerling-Zheng  
S. Kloska  
T. Engelhorn  
C.M. Strother  
W.A. Kalender  
M. Köhrmann  
S. Schwab  
A. Doerfler



# Flat Detector CT in the Evaluation of Brain Parenchyma, Intracranial Vasculature, and Cerebral Blood Volume: A Pilot Study in Patients with Acute Symptoms of Cerebral Ischemia

**BACKGROUND AND PURPOSE:** The viability of both brain parenchyma and vascular anatomy is important in estimating the risk and potential benefit of revascularization in patients with acute cerebral ischemia. We tested the hypothesis that when used in conjunction with IV contrast, FD-CT imaging would provide both anatomic and physiologic information that would correlate well with that obtained by using standard multisection CT techniques.

**MATERIALS AND METHODS:** Imaging of brain parenchyma (FD-CT), cerebral vasculature (FD-CTA), and cerebral blood volume (FD-CBV) was performed in 10 patients. All patients also underwent conventional multisection CT, CTA, CTP (including CBV, CTP-CBV), and conventional catheter angiography. Correlation of the corresponding images was performed by 2 experienced neuroradiologists.

**RESULTS:** There was good correlation of the CBV color maps and absolute values between FD-CBV and CTP-CBV (correlation coefficient, 0.72;  $P < .001$ ). The Bland-Altman test showed a mean difference of CBV values between FD-CT and CTP-CBV of  $0.04 \pm 0.55$  mL/100 mL. All vascular lesions identified with standard CTA were also visualized with FD-CTA. Visualization of brain parenchyma by using FD-CT was poor compared with that obtained by using standard CT.

**CONCLUSIONS:** Both imaging of the cerebral vasculature and measurements of CBV by using FD-CT are feasible. The resulting vascular images and CBV measurements compared well with ones made by using standard CT techniques. The ability to measure CBV and also visualize cerebral vasculature in the angiography suite may offer significant advantages in the management of patients. FD-CT is not yet equivalent to CT for imaging of brain parenchyma.

**ABBREVIATIONS:** CBF = cerebral blood flow; CBV = cerebral blood volume; CTA = CT angiography (IV contrast); CTP = perfusion multisection CT; CTP-CBV = perfusion multisection CT cerebral blood volume (IV contrast); DSA = digital subtraction angiography; DWI = diffusion-weighted imaging; FD = flat detector; FD-CBV = flat detector cerebral blood volume (IV contrast); FD-CT = flat detector CT; FD-CTA = flat detector CT angiography (IV contrast); HU = Hounsfield unit; ICA = internal carotid artery; IV = intravenous; MCA = middle cerebral artery; MIP = maximum intensity projection; MPR = multiplanar reconstruction; MSCT = multisection CT; MTT = mean transit time; PWI = perfusion-weighted imaging; TIA = transient ischemic attack; TTP = time-to-peak; VA = vertebral artery

Recently, FD-equipped angiography machines are increasingly used for neuroangiographic imaging.<sup>1</sup> Using this equipment, it is now possible to obtain not only high-quality 3D vascular volumes (3D rotational angiography) but also CT-like images (FD-CT) of brain parenchyma that allow detection of intraparenchymal and subarachnoid hemorrhages.<sup>2-7</sup>

In FD-CT, a volume of interest is imaged using a rotational acquisition over an angular range of about 200°. From this, a series of 2D projection images (“frames”) are obtained and are then reconstructed using a CT-like algorithm to create a 3D volume that can be post-processed for visualization and anal-

ysis like conventional multisection CT images.<sup>8</sup> Using this technique, CT images of the brain can be obtained without the need to transfer patients from the angiography suite to a CT facility.<sup>9</sup> FDs, like those used in this study, offer a low contrast resolution with demonstrated ability for recognition of contrast differences as little as 10 HU.<sup>10</sup> But low contrast resolution is still inferior in comparison to multisection CT. However, this capability has already been shown to enhance the ability to rapidly recognize and manage some intra-procedural complications.<sup>3-6</sup>

Along with the FD-CT has been the rapid development of new stents and mechanical recanalization devices, which provide a means to achieve rapid and effective revascularization or recanalization in patients with acutely symptomatic arterial stenosis or occlusion.<sup>11-14</sup> Because these devices are used more and more and because evidence suggests that early reperfusion is one factor associated with a good clinical outcome, it is crucial for techniques to minimize the time required from presentation at an acute care facility to diagnosis and treatment of those patients who may benefit from early intervention.<sup>15</sup> The assessment of the impact of an ischemic insult on

Received October 19, 2009; accepted after revision February 2, 2010.

From the Department of Neuroradiology (T.S., S.K., T.E., A.D.), Institute of Medical Physics (W.A.K.), and Department of Neurology (M.K., S.S.), University of Erlangen-Nuremberg, Erlangen, Germany; Siemens AG (Y.D.-Z.), Healthcare Sector, Forchheim, Germany; and Department of Radiology (C.M.S.), University of Wisconsin Hospitals and Clinics, Madison, Wisconsin.

Please address correspondence to Arnd Doerfler, MD, PhD, Department of Neuroradiology, University of Erlangen-Nuremberg, Schwabachanlage 6, 91054 Erlangen, Germany; e-mail: arnd.doerfler@uk-erlangen.de

DOI 10.3174/ajnr.A2083

brain viability is best performed by using physiologic rather than morphologic criteria, especially in the acute phase when morphologic changes are absent or minimal and, at the same time, options for interventions aimed at tissue salvage are greatest and most effective.<sup>16–18</sup> Until now, this assessment has been done by using multitechnique CT (CT, CTA, CTP) and MR imaging (PWI, DWI).<sup>19–24</sup>

If on the basis of these images, a decision is made to attempt interventional revascularization, then an additional time-consuming patient transfer to the angiography suite is necessary. The ideal setting in which to evaluate a patient with an acute ischemic stroke would be an imaging environment in which assessment of parenchyma, vasculature, and perfusion and, if indicated, treatment could be undertaken (ie, the angiography suite). This would avoid the need for time-consuming transfer from one technique to another. In addition, monitoring of brain perfusion during endovascular procedures may add further value in decision-making regarding when to continue or to abort further attempts at revascularization.<sup>25</sup> This would require an FD-CT program offering parenchymal, angiographic, and perfusion images.

Although currently available FD-CT systems do not provide the necessary temporal resolution to assess CBV or TTP, there is evidence that they do provide a means to measure CBV levels at an accuracy comparable with that of CTP.<sup>26–28</sup> Postprocessing of this special data acquisition should also provide visualization of the brain and vasculature.

In this study, we tested the hypothesis that acquisition of a whole-brain FD-CT volumetric soft-tissue volume obtained in conjunction with the IV injection of contrast media would provide an imaging dataset that would allow depiction of brain parenchyma, cerebral vasculature, and CBV comparable with that obtained by using standard multisection CT techniques.

## Materials and Methods

Ethics committee approval was obtained before this study, and all patients gave written informed consent. We prospectively included 10 patients (4 women, 6 men) with acutely symptomatic intracranial ( $n = 5$ ) or extracranial ( $n = 1$ ) stenosis or an acute ischemic stroke due to an intracranial arterial occlusion ( $n = 2$ ). Two patients presenting with TIA were found to have incidental aneurysms ( $n = 2$ ). All patients were evaluated by multitechnique imaging including conventional CT (CT, CTA, CTP-CBV), FD-CT (FD-CT, FD-CTA, FD-CBV), and conventional angiography (DSA). All patients were examined by conventional CT on admission and were then scheduled for DSA and FD-CT evaluation within 12–24 hours after admission. According to institutional guidelines, all patients were also scheduled for routine follow-up imaging (CT or MR imaging) 24–48 hours after admission.

## Imaging Protocol

**Multisection CT.** Conventional multisection CT was performed on a 64-section CT scanner (Somatom 64; Siemens, Forchheim, Germany). We obtained routine CT images of the skull base and supratentorial structures with the following parameters: skull base: collimation,  $12 \times 1.2$  mm; 120 kV; 380 mAs; reconstructed section width, 4.8 mm; kernel, H31s; cerebrum: collimation,  $24 \times 1.2$  mm; 120 kV; 400 mAs; reconstructed section width, 7.2 mm; kernel, H31s. Using

bolus tracking, CTA was performed with a standard protocol using the following parameters: collimation,  $64 \times 0.6$  mm; 120 kV; 160 mAs; kernel, B20f; pitch, 1.3; reconstruction increment, 0.4. Using these parameters, the effective patient dose was approximately 17.8 mSv (2.8 mSv CT, 3 mSv CTA, 12 mSv CTP; information provided by Siemens). Sixty milliliters of contrast medium (Iomeprol, Imeron 350; Bracco Imaging, Konstanz, Germany) was injected into a peripheral vein at a rate of 4 mL/s, followed by a 60-mL saline flush. CTP imaging was performed with a standard protocol by using the following parameters: 3 sections at the level of the basal ganglia including obtaining 1 scan per second during 40 seconds at 80 kV and 270 mAs. A collimation of  $24 \times 1.2$  mm was chosen with a section thickness of 9.6 mm. The dynamic scan started 10 seconds after the injection of 40 mL of contrast medium (Imeron 350) at 6 mL/s followed by a 60-mL saline flush. The contrast medium was injected into a peripheral vein through an 18-gauge catheter (Vasofix Safety; Braun Melsungen, Melsungen, Germany). Contrast medium was injected by using a dual-syringe power injector (Medtron, Saarbruecken, Germany).

**Postprocessing of Multisection CT Images.** Semiautomated analysis of the CTP data was performed on a standard workstation (syngo MultiModality Workplace, Siemens) by using standard CTP software. Color-coded perfusion parameter maps including CBV were calculated by using a previously described method.<sup>29</sup> The CTA dataset was reconstructed in MIPs in axial (20-mm section thickness; distance, 5 mm), coronal (10-mm section thickness; distance, 5 mm), and oblique (5-mm section thickness; distance, 3 mm) planes adjacent to a stenosis or occlusion.

**FD-CT.** FD-CT imaging was performed on a biplane FD angiographic system (Axiom Artis dBA, Siemens). The acquisition consisted of 2 rotations: an initial rotation (mask run) followed by a second rotation after appropriate contrast medium injection (fill run). Data acquisition per run was performed by using the following parameters: acquisition time, 8 seconds; 70 kV;  $616 \times 480$  matrix; projection on  $30 \times 40$  cm flat panel size;  $200^\circ$  total angle;  $0.5^\circ$  per frame; 400 frames total; dose, 0.36 mGy per frame.

Because of a lack of temporal resolution caused by the limited speed of gantry movement, CBV can only be obtained by using a contrast medium injection protocol that results in a steady state of contrast medium in the brain parenchyma during acquisition of the fill run. Because bolus tracking is not available with FD-CT imaging, we used a different technique to detect a proper time point to start the fill run acquisition. Contrast medium injection was started simultaneously with the start of the mask run. After the mask run acquisition was completed, the C-arm returned to the start position. Combined, this requires an interval of 13 seconds. When the C-arm returned to its original (start) position, standard 2D-DSA acquisitions were then initiated at the rate of 2 images per second. When the operator observed opacification of the transverse sinus, there was assumed to be a steady state of contrast medium in the brain parenchyma and the second rotation (fill run) was then manually initiated (bolus watching). The time delay between initial injection of the contrast medium and the start of the second rotation varied between 16 and 19 seconds. This corresponds to that described in earlier experimental studies.<sup>23,24</sup> Eighty milliliters of contrast medium (Imeron 350, Bracco Imaging) was injected into a peripheral vein at a rate of 4 mL/s by using a power injector (Mark V ProVis; Medrad, Indianola, Pennsylvania).

## Postprocessing of FD-CT Imaging

**Parenchymal and Vascular Imaging (FD-CT).** Postprocessing of the FD-CT dataset was performed on a commercially available dedicated workstation (Leonardo DynaCT, InSpace 3D software; Siemens). The software includes application of system-specific filter algorithms to correct for beam hardening, scattered radiation, truncated projections, and ring artifacts. The software allows different algorithms to be used so that reconstructions can be done of only the mask run (analogous to a noncontrast CT scan) and only of the fill run (analogous to CTA).

Postprocessing of the mask run results in a volume dataset with a batch of about 400 sections, 0.36-mm thickness in a  $512 \times 512$  matrix format. Reconstructions were performed using kernel-type “HU”, image-impression “smooth,” FOV of 18 cm and a reconstruction-mode “native mask” (eg, reconstruction of the mask run only to visualize the brain parenchyma). The dataset was then further processed as MPRs with 4.8- and 7.2-mm section thicknesses. Images were viewed in an axial orientation. The orientation and location of these MPR sections were matched with ones from the CT and were used to analyze the status of the brain parenchyma.

Additional reconstruction of the fill run was performed using a reconstruction-mode “native fill” (to visualize vascular structures), kernel-type “HU”, image-impression “normal” and FOV of 14 cm. Reconstruction of raw data resulted in a volume dataset with a batch of approximately 400 sections with a single section thickness of 0.22 mm. MIP reconstructions were matched with ones from the CTA for comparison.

**Perfusion Imaging (FD-CBV).** FD-CT CBV postprocessing was performed by using prototype software installed on a research workstation (Syngo XWP, Siemens). For this, we used a postprocessing algorithm identical to that previously described.<sup>27,28</sup> Briefly, the mask and the fill run were reconstructed and subtracted. An algorithm to segment out air and bone was applied. The steady state arterial input function value was then calculated from an automated histogram analysis of the vessel tree. A final scaling was then applied to the dataset to account for the arterial input value. In a final step, a smoothing filter was applied to reduce pixel noise. In contrast to CT, the FD-CT CBV acquisition provides coverage of the entire brain. To compare the FD-CT CBV maps with those from CTP-CBV, we reconstructed 3 sections by using MPR, 9.6-mm section thickness. For comparison, these reconstructions were matched for position and angulation with those obtained by using CTP-CBV.

## Data Analysis

All images were stored on a workstation for analysis. Image comparison was performed by 2 experienced neuroradiologists unaware of patient history. Statistical analysis was performed by using the Statistical Package for the Social Sciences, Version 14.0 (SPSS, Chicago, Illinois).

## Parenchymal Imaging

Conventional CT and FD-CT images matched as closely as possible for section level and angulation were independently reviewed. The reviewers were asked to report on the presence of classic signs of infarction like hypoattenuating or hyperattenuating vascular segments.<sup>30</sup> Ventricular size was estimated by the Evans index.<sup>4,31</sup>

## Vascular Imaging

Review of the CTA and FD-CTA images was performed with the reviewers noting the presence of any vascular pathology (eg, occlu-

sions or stenosis). The reviewers were asked specifically to evaluate the MCA (M1, M2), the intracranial segment of the VAs (V4), the basilar artery, and the posterior cerebral arteries (P1, P2). As has been previously described, they performed measurements of any stenosis seen on images from any of the modalities: percent stenosis =  $\{[1 - (D \text{ stenosis} / D \text{ normal})]\} \times 100$ . D stenosis is the diameter of the diseased segment at its most severe site. D normal is the diameter of the normal artery proximal to the stenosis.<sup>32</sup> The DSA images were also available for review and served as the criterion standard.

## Perfusion Imaging

Six anatomic regions were defined for CBV measurement (Fig 1A). These were chosen to include both white and gray matter:

- 1) Lateral basal ganglia (4 cm<sup>2</sup>).
- 2) Frontal subcortical white matter (3 cm<sup>2</sup>).
- 3) Occipital subcortical white matter (3 cm<sup>2</sup>).
- 4) Thalamus (2.5 cm<sup>2</sup>).
- 5) Corona radiata (7 cm<sup>2</sup>).
- 6) Internal capsule, posterior limb (1.5 cm<sup>2</sup>).

As closely as possible, the CTP-CBV maps and the FD-CT CBV maps of each patient were registered manually so that the anatomic regions were the same. Regions of interest were then placed manually in each of the defined regions. We did not place regions of interest in the cortex because our preliminary experience indicated that this could include vessels of the subarachnoid space within the regions of interest, which could then distort the measurements. For each of the 12 regions of interest (96 pairs of data points in all patients) on both hemispheres, the mean CBV values were recorded. Thus 16 data points for each of the 6 anatomic regions were obtained.

## Statistics

Statistical analysis was performed as follows: We calculated the Pearson correlation coefficient between the CTP-CBV and FD-CT CBV values. If a CTP-CBV map showed a lesion, this region was measured in the corresponding FD-CT CBV map and was reported separately (Table). We calculated mean CBV values for each region of interest and then calculated the correlation coefficient between CTP-CBV and FD-CT CBV values. For assessment of agreement between the 2 methods of clinical measurements, we used Bland-Altman analysis (Fig 1).<sup>33</sup>

## Results

All FD-CT studies were obtained within 24 hours (mean,  $17.2 \pm 2.8$  hours, Table) of the initial CT examination. FD-CT, CT, and DSA were feasible, and acquisition of all parameters was possible in all patients.

## Parenchymal Imaging

Comparison of CT and FD-CT images demonstrated that the ventricles could be well visualized on both modalities, with the Evans index being identical with measurements from CT or FD-CT (Table). In 7 patients, there was no evidence of ischemic stroke visible on any technique, including follow-up CT or MR imaging performed 24 hours after the initial assessments (patients 1, 2, 4, 5, 6, 9, 10). In the 3 patients (patients 3, 7, 8) with an area of demonstrated ischemia on CT, the FD-CT image quality was not sufficient to visualize an abnormality. At the start of the study, we recognized that the image quality of FD-CT was not suffi-



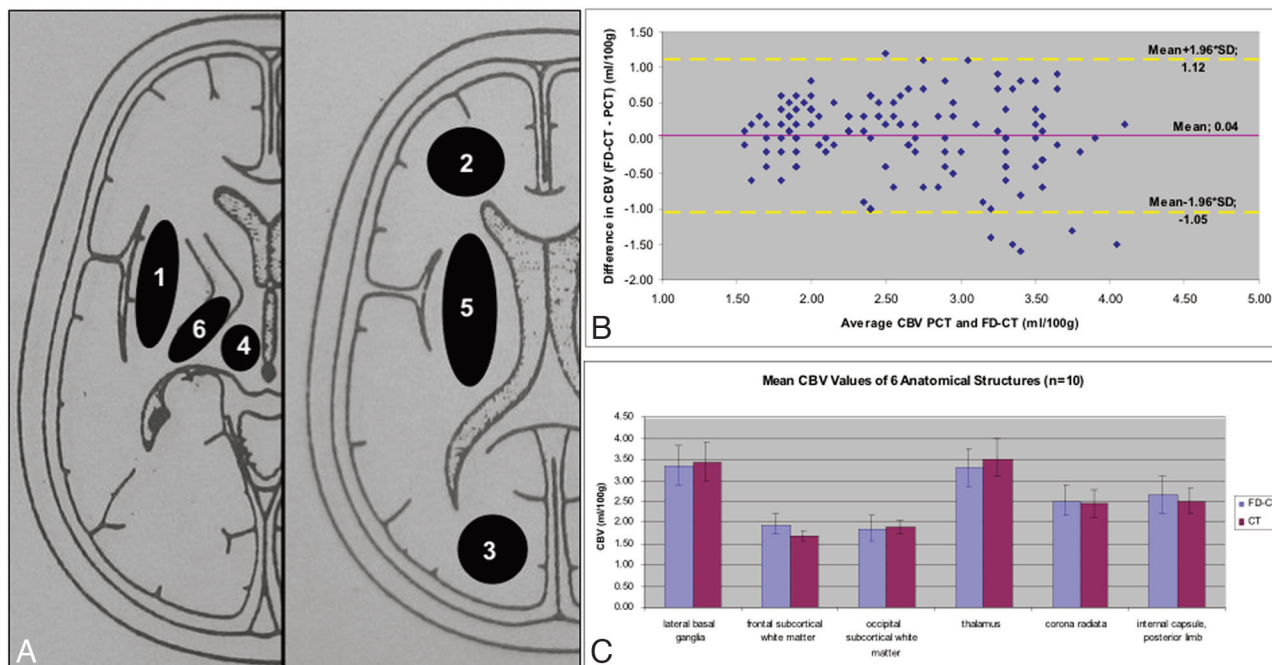


**Fig 1.** A, Regions of interest for CBV measurements: 1) lateral basal ganglia; 2) frontal subcortical white matter; 3) occipital subcortical white matter; 4) thalamus; 5) corona radiata; 6) internal capsule, posterior limb. B, Bland-Altman plot displays slightly higher FD-CBV values (0.04 mL/100 mL) in comparison with CTP. C, Mean CBV values and SDs of the 6 regions of interest show only minimal deviations.

#### Summary of clinical and imaging characteristics

No.	Age (yr)	Vascular Pathology	Symptoms	Treatment	CBV Lesion	FD-CT CBV	CTP-CBV	Evans Index		Stenosis Grade (%)			Interval, CT to FD-CT (hr)
								FD-CT	MSCT	FD-CT	MSCT	DSA	
1	81	VA stenosis, right	TIA	Medical				0.27	0.28	67	66	72	20.5
2	70	Extracranial ICA stenosis	TIA	Carotid stenting				0.26	0.25				17.75
3	76	MCA occlusion, left	Minor stroke	Medical	Internal capsule, anterior limb	2.6 mL/100 mL	2.7 mL/100 mL	0.31	0.32				18
4	61	MCA stenosis, left	TIA	Stent				0.42	0.43	94	92	95	16.5
5	61	VA stenosis, left	TIA	Medical				0.37	0.36	82	78	80	18.5
6	69	VA stenosis, right	TIA	Medical				0.3	0.31	88	85	84	13.5
7	50	MCA stenosis, right	Minor stroke	Stent	Internal capsule, anterior limb	2.1 mL/100 mL	1.8 mL/100 mL	0.25	0.26	80	81	76	13.75
8	52	MCA occlusion, right	Minor stroke	Medical	Temporal lobe	1.6 mL/100 mL	Not visible	0.21	0.22				16.25
9	67	MCA aneurysm	TIA	Medical				0.28	0.27				14.5
10	67	Carotid aneurysm	TIA	Medical				0.24	0.25				21.5

cient to allow recognition of signs of acute stroke such as hypoattenuation, focal swelling, or hyperattenuated vascular segments. For this reason, further evaluation by using an Alberta Stroke Program Early CT Score scale to compare FD-CT with CT was not initiated.

#### Vascular Imaging

Review of the MIP reconstructions of the vascular images from both FD-CTA and CTA as well as the DSA images revealed that all intracranial vascular lesions seen on the DSA and CTA could also be visualized on the FD-CTA images (Fig 2 C, -D). One patient had a high-grade (>95%) stenosis of the cervical segment of the internal carotid artery visible on CTA of the neck. FD-CTA of the neck was not performed, so this lesion was not included in our evaluation. Both reviewers recognized all lesions on the FD-CTA that were identified on images from the DSA or the CTA. There was a subjective opinion by the reviewers that the image quality of FD-CTA com-

pared with that of CTA was at least identical and perhaps superior. Measurement of the degree of stenosis was identical when made on the CTA, FD-CTA, and DSA images (Table). In 2 subjects (patients 9 and 10) presenting with TIA, aneurysms were detected on both CTA and FD-CTA. Lumbar puncture could rule out subarachnoid hemorrhage in both, so both aneurysms were incidental ones. Arterial stenosis or occlusions were not visible in these 2 patients.

#### Perfusion Imaging

Using our technique for timing the contrast bolus for the FD-CBV acquisition (bolus watching), all acquisitions were successful. None had to be repeated. It was feasible to measure CBV in all FD-CBV data sets so that both the CTP-CBV and the FD-CBV image and data quality were suitable for evaluation in all patients. There was good correlation of CBV color maps between FD-CBV and CTP-CBV (Fig 2A, -B). Abnormalities were found on the CBV maps from both modalities in

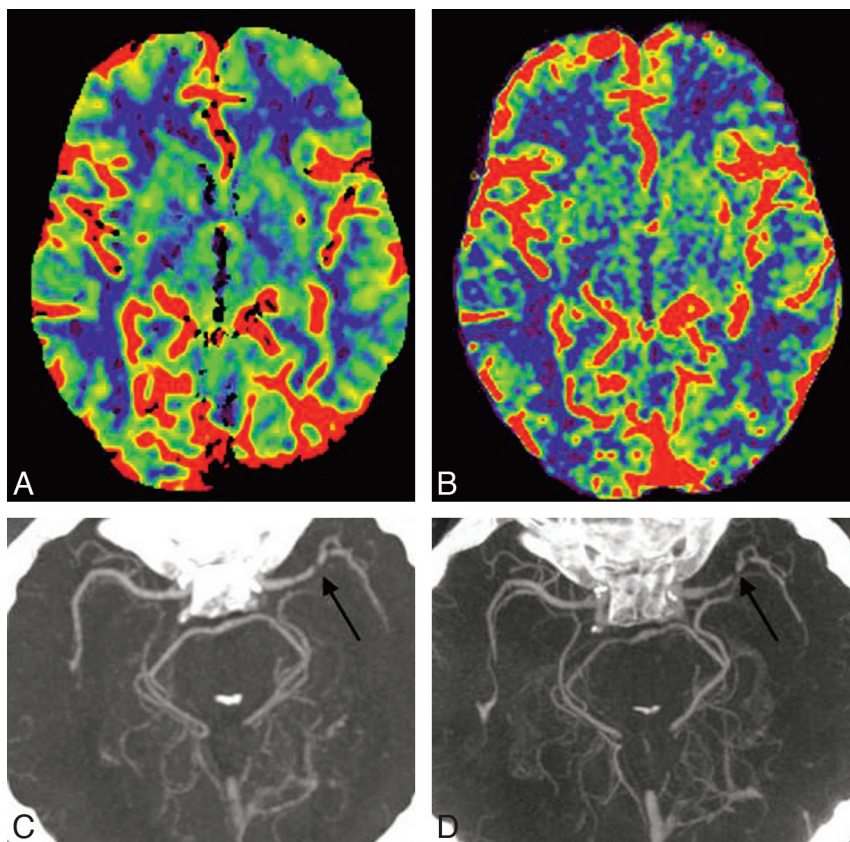


**Fig 2.** CT (A) and FD-CT (B) show the good correlation of CBV color maps. CTA (C) and FD-CTA (D) display a high-grade stenosis (black arrows) of the left MCA (patient 4). Note the perfect delineation of this high-grade stenosis in FD-CTA.

2 of the 10 patients (patient 3, 7). In these 2 patients, CBV abnormalities were secondary to ischemia. In 1 additional patient (patient 8), a CBV abnormality was detected on the FD-CBV map. The CBV maps from the CTP study did not include this area of the brain (temporal lobe), thus making it impossible to compare these 2 studies. The results from the CBV studies in these 3 patients are given in the Table. In patient 8, the CBV value within the lesion was 1.6 mL/100 mL; in the same region of the opposite hemisphere, it was 3.1 mL/100 mL. A subsequent CT scan confirmed an infarct in the region of abnormality seen on the FD-CBV map.

The Bland-Altman test<sup>33</sup> in Fig 1B showed that the mean difference of CBV values between FD-CT and CTP was  $0.04 \pm 0.55$  mL/100 mL, meaning that FD-CBV values were slightly higher than CTP values. The mean and SD of the CBV values in each of the 6 anatomic regions among the 10 patients are shown in Fig 1C. The mean values show only minimal differences, and the SDs overlap widely. The correlation coefficient between the CTP-CBV and FD-CT CBV values of all the regions of interest was 0.72 ( $P < .001$ ).

### Illustrative Case

A 50-year-old man (patient 7) presenting with signs of a right MCA stroke was admitted as an emergency (Figs 3 and 4). CT, CTA, and CTP-CBV revealed a high-grade MCA stenosis and a decrease in CBV in the region of the anterior limb of the internal capsule. MR imaging 24 hours later demonstrated a region of ischemic injury involving the anterior limb of the internal capsule matching with the CBV deficit seen on the

CTP-CBV examination. DSA and FD-CTA performed 24 hours after admission confirmed a high-grade M1 stenosis. The area of infarction was faintly visible on the FD-CT; however, the FD-CTA clearly demonstrated the high-grade MCA stenosis and the FD-CBV map was identical to that obtained with the CTP-CBV technique. Measurement of CBV values of the affected region was 1.8 mL/100 mL in the CTP-CBV study and 2.1 mL/100 mL in FD-CT CBV study.

### Discussion

Our study demonstrates the feasibility of FD-CT in conjunction with IV administration of contrast medium to obtain images of brain parenchyma, brain vasculature, and CBV maps in patients with cerebrovascular diseases in the angiography suite. The potential of this technique to shorten the time from when a patient with an acute ischemic stroke is first seen at a hospital to the time when a definitive diagnosis and therapeutic decision can be made seems obvious. Application of this approach would improve clinical workflow and would offer potential improvements in both the safety and efficacy of endovascular treatments because time-consuming and potentially dangerous transportations may be avoided.<sup>18,34</sup>

At the moment, because of lack of temporal resolution of FD-CT, a full assessment of brain perfusion with all parameters cannot be performed. The ability to obtain CBV values that, in our study and in experimental studies by others, correspond well with those made by using CTP techniques does provide, however, a way to assess the status of brain viability of patients in the angiography suite.<sup>27,28</sup> With CT or MR imaging

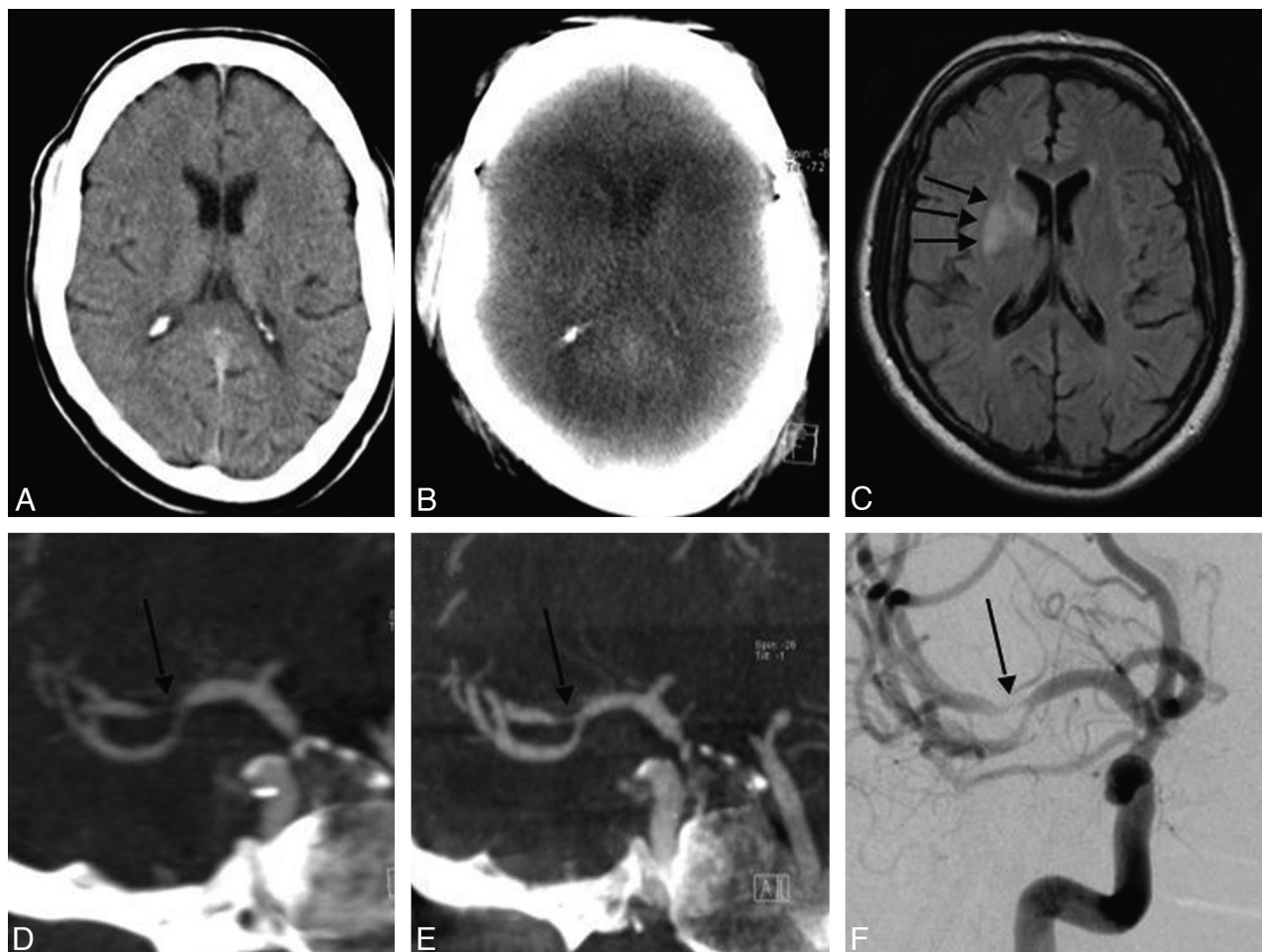


**Fig 3.** *A*, At initial scanning, the brain appears without any signs of stroke. *B*, FD-CT performed 24 hours later cannot visualize the stroke region. *C*, MR imaging also performed 24 hours later confirms infarct demarcation (*arrows*). *D–F*, MIP reconstruction of the CTA (*D*) and FD-CTA (*E*) corresponds perfectly with the DSA finding (*F*) of stenosis (*arrow*) in the distal M1 as well as the proximal M2 segments. Notice the sharp delineation of the vessels in FD-CTA in contrast to that in CTA.

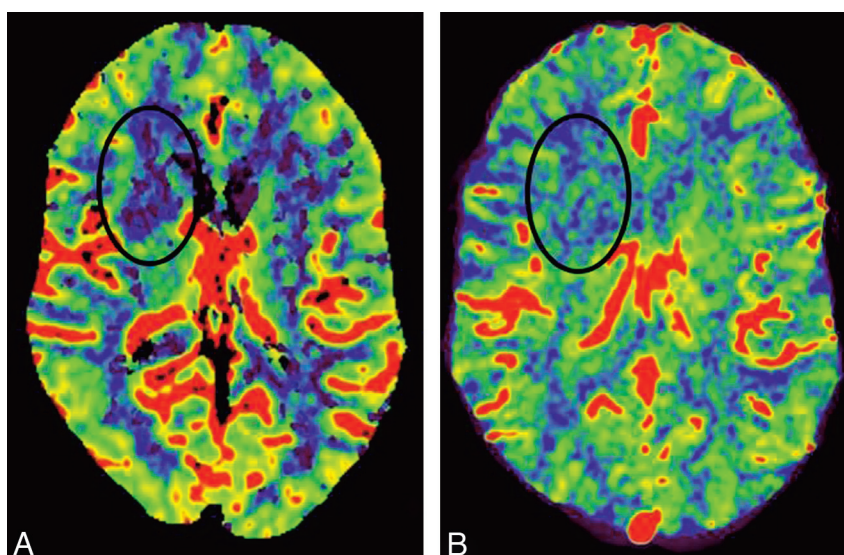


**Fig 4.** *A* and *B*, Comparison of CTP-CBV (*A*) with FD-CBV (*B*) demonstrates decrease of CBV in the region of the internal capsule, anterior limb. *C*, The region matches nicely with the MR image (Fig 3*C*).

in the triage of patients admitted with symptoms of acute ischemic stroke, calculation of CBV is the most important parameter for determining whether autoregulation is still in-

tact.<sup>25,34–36</sup> Also, in humans, there is some evidence to indicate that the perfusion parameter that best describes the infarct core is the absolute CBV. Using CT in combination with CBV



values from CTP, Parsons et al<sup>35</sup> demonstrated the ability to distinguish ischemic but salvageable tissue (eg, penumbra) from ischemic and nonviable tissue (eg, infarct core). These studies confirm our opinion as to the potential value of this technique and correlate well with assessments of brain viability made in our 3 patients with obvious abnormalities in their CBV values. Ischemic lesions on CTP-CBV in our patients were also demonstrated on the FD-CBV studies with good correlation of both qualitative color maps and absolute numbers between the 2 techniques. In 1 of the 3 patients (patient 8), the lesion was only recognized on the FD-CBV map because of lack of adequate brain coverage with the CTP-CBV technique. Full brain coverage is an obvious advantage of FD-CBV.

Another advantage of the technique that we describe is the potential for reduction in the amount of contrast medium and the dose of radiation needed for patient evaluation. Using FD-CT, one can obtain both a FD-CTA and a FD-CBV measurement from a single acquisition. In contrast, 2 acquisitions and 2 injections of contrast medium are required to obtain the same data by using conventional CT. In our study, all vascular lesions were recognized in FD-CTA images. The image quality of the FD-CTAs appeared comparable with that of the CTAs.

Our preliminary results show clearly that the FD-CT images are not of sufficient quality to allow an assessment of the brain parenchyma for signs of ischemia. In our 3 patients in whom CT or MR imaging follow-up could clearly demonstrate infarction, these regions could not be recognized on the FD-CT images. Thus, currently FD-CT does not provide image quality that is adequate for initial diagnostic evaluation of patients with a suspected acute ischemic stroke. So far publications addressing the visibility of hemorrhages are available, but there are, to our knowledge, no publications concerning the visibility of ischemic areas.<sup>5-8</sup> Concerning radiation dose, our acquisition protocol for the FD-CT is a low-dose protocol with approximately 1.0-mSv effective dose in comparison with CT (17.8 mSv). High-dose FD-CT protocols are available and need to be evaluated in regard to how a higher dose might improve the ability to visualize signs of ischemic injury. Even with a higher dose, however, FD image quality, sufficient to compete with standard CT, will require significant improvements in the ability to reduce scatter radiation, eliminate beam hardening artifacts, and reduce the artifacts caused by patient motion.

Our study has several shortcomings. First, the number of patients was small, and the patient population was heterogeneous. While this precludes a clear determination of the value that FD techniques may offer over conventional methods, we believe that our study is sufficient to show feasibility and also to encourage other authors to explore the use of this technology. Second, it is unproven whether the ability to measure CBV without concomitant measurement of CBF and MTT will allow accurate determination of the viability of brain parenchyma. Prior work has compared and discussed the value of the 3 parameters in detail.<sup>27-29</sup> Because of the 3 parameters, CBV is the one most useful in determining whether autoregulation is still intact (and thus parenchyma is still salvageable), we believe that the ability to assess this single parameter, in the angiographic suite during an attempt at revascularization, will

add value to the management of patients with acute ischemia. Clearly, further work is required to confirm our opinion. Finally, because of the limited scope of pathology present in our patients, we cannot comment on how FD-CTA will compare with CTA for the evaluation of other vascular conditions, (eg, normal vasculature or arteriovenous malformations).

A critical point in obtaining reliable vascular images and CBV maps with FD-CT is the timing of the injection and the amount of the contrast medium used. In the absence of established protocols, we had to rely on initial animal studies.<sup>27,37</sup> Bolus watching seems to provide the best chance to ensure that the fill run is acquired during a steady state of parenchymal opacification while still minimizing the amount of contrast medium that is used. Therefore we used 80 mL of contrast material without a saline chase. By using a dual-syringe injection system, the contrast bolus might be made more compact and also reduced in volume. Optimized protocols by using dual-syringe injection systems will be the topic of further research.

In addition, FD-CT imaging may be useful during treatment procedures. The ability to monitor tissue viability sequentially during such treatments might also improve safety, by improving the ability to stop an intervention when there has been a significant increase in nonviable tissue since initial evaluation. Finally, if it is possible to document the treatment result at the end of the procedure, control CT or MR imaging may then be scheduled for the next 24–48 hours or on demand if patient condition should deteriorate.

Another future application that may benefit from this FD-CT protocol is monitoring of endovascular therapy of cerebral vasospasm, especially if measurements of CBF and TTP should be possible in future by using faster rotating C-arm systems.<sup>38</sup> Also there is evidence that CBV maps obtained with high-resolution imaging could add value to planning and performing a biopsy in patients with brain tumors.<sup>39</sup>

Further investigations are necessary to confirm our preliminary results in this small group of patients. We think, however, that by combining the imaging and postprocessing techniques that we describe, an FD-CT multimodal imaging protocol suitable for initial assessment of patients with acute ischemia is feasible. To realize this, however, techniques that provide improved soft-tissue resolution equivalent to that of conventional CT and temporal resolution adequate to assess CBF and MTT must be developed. Efforts are ongoing to resolve these limitations.

## Conclusions

Imaging of both the cerebral vasculature and CBV by using FD-CT is feasible and can be done by using a single IV injection of contrast medium. Vascular images and CBV measurements compared well with ones made by using standard CT and DSA. Image quality of this FD-CT program was not sufficient to recognize signs of ischemia. The ability to measure CBV and to image cerebral vasculature by using an IV injection of contrast medium within the angiographic suite may significantly improve the management of patients with acute ischemic strokes.



## References

- Fahrig R, Fox S, Lownie S, et al. Use of a C-arm system to generate true 3-D computed rotational angiograms: preliminary in vitro and in vivo results. *AJNR Am J Neuroradiol* 1997;18:1507–14
- Kalender W, Kyriakou Y. Flat-detector CT (FD-CT). *Eur Radiol* 2007;17:2767–79
- Akpek S, Brunner T, Benndorf G, et al. Three-dimensional imaging and cone beam volume CT in C-arm angiography with flat panel detector. *Diagn Interv Radiol* 2005;11:10–13
- Heran NS, Song JK, Namba K, et al. The utility of DynaCT in neuroendovascular procedures. *AJNR Am J Neuroradiol* 2006;27:330–32
- Doelken M, Struffert T, Richter G, et al. Flat-panel detector volumetric CT for visualization of subarachnoid hemorrhage and ventricles: preliminary results compared to conventional CT. *Neuroradiology* 2008;50:517–23
- Struffert T, Richter G, Engelhorn T, et al. Visualisation of intracerebral haemorrhage with flat-detector CT compared to multislice CT: results in 44 cases. *Eur Radiol* 2009;19:619–25
- Engelhorn T, Struffert T, Richter G, et al. Flat-panel detector angiographic CT in the management of aneurysmal rupture during coil embolization. *AJNR Am J Neuroradiol* 2008;29:1581–84
- Söderman M, Babic D, Holmin S, et al. Brain imaging with a flat detector C-arm: technique and clinical interest of XperCT. *Neuroradiology* 2008;50:863–68
- Kamran M, Nagaraja S, Byrne JV. C-arm flat detector computed tomography: the technique and its applications in interventional neuro-radiology. *Neuroradiology* 2010;52:319–27
- Zellerhoff M, Scholz B, Röhrnschopf E. Low contrast 3D-reconstruction from C-arm data. *Progress Biom Opt Imag Proc SPIE* 2005;5745:646–55
- Smith WS, Sung G, Starkman S, et al. Safety and efficacy of mechanical embolectomy in acute ischemic stroke: results of the MERCI trial. *Stroke* 2005;36:1432–38
- Bose A, Henkes H, Alfke K, et al. The Penumbra System: a mechanical device for the treatment of acute stroke due to thromboembolism. *AJNR Am J Neuroradiol* 2008;29:1409–13
- The Penumbra Pivotal Stroke Trial Investigators. The Penumbra Pivotal Stroke Trial: safety and effectiveness of a new generation of mechanical devices for clot removal in intracranial large vessel occlusive disease. *Stroke* 2009;40:2761–68. Epub 2009 Jul 9
- Struffert T, Köhrmann M, Engelhorn T, et al. Penumbra Stroke System as an “add-on” for the treatment of large vessel occlusive disease following thrombolysis: first results. *Eur Radiol* 2009;19:2286–93
- Jansen O, Schellinger P, Fiebach J, et al. Early revascularization in acute ischemic stroke saves tissue at risk defined by MRI. *Lancet* 1999;353:2036–37
- Hamberg LM, Hunter GJ, Kierstead D, et al. Measurement of cerebral blood volume with subtraction three-dimensional functional CT. *AJNR Am J Neuroradiol* 1996;17:1861–69
- Wintermark M, Flanders AE, Velthuis B, et al. Perfusion-CT assessment of infarct core and penumbra: receiver operating characteristic curve analysis in 130 patients suspected of acute hemispheric stroke. *Stroke* 2006;37:979–85
- Saver JL. Time is brain: quantified. *Stroke* 2006;37:263–67
- Schellinger PD, Fiebach JB, Hacke W. Imaging-based decision making in thrombolytic therapy for ischemic stroke: present status. *Stroke* 2003;34:575–83
- Warach S, Dashe JF, Edelmann RR. Clinical outcome in ischemic stroke predicted by early diffusion-weighted and perfusion magnetic resonance imaging: a preliminary analysis. *J Cereb Blood Flow Metab* 1996;16:53–59
- Wintermark M, Fischbein NJ, Smith WE, et al. Accuracy of dynamic perfusion-CT with deconvolution in detecting acute hemispheric stroke. *AJNR Am J Neuroradiol* 2005;26:104–12
- Furlan A, Higashida R, Wechsler L, et al. Intra-arterial prourokinase for acute ischemic stroke: the PROACT II study—a randomized controlled trial. Prol-ysin in Acute Cerebral Thromboembolism. *JAMA* 1999;282:2003–11
- IMS II Trial Investigators. The Interventional Management of Stroke (IMS) II Study. *Stroke* 2007;38:2127–35. Epub 2007 May 24
- Chalela JA, Kidwell CS, Nentwich LM, et al. Magnetic resonance imaging and computed tomography in emergency assessment of patients with suspected acute stroke: a prospective comparison. *Lancet* 2007;369:293–98
- Heidenreich JO, Hsu D, Wang G, et al. Magnetic resonance imaging results can affect therapy decisions in hyperacute stroke care. *Acta Radiol* 2008;49:550–57
- Zellerhoff M, Deuerling-Zheng Y, Strother CM, et al. Measurement of cerebral blood volume using angiographic C-arm systems. Zellerhoff M, Deuerling-Zheng Y, Strother CM, et al, eds. In: *Medical Imaging 2009: Biomedical Applications in Molecular, Structural, and Functional Imaging*. Vol.7261. Bellingham, Washington: Society of Photo-Optical Instrumentation Engineers; 2009:72620H-72620H-8
- Ahmed AS, Zellerhoff M, Strother CM, et al. C-arm CT measurement of cerebral blood volume: an experimental study in canines. *AJNR Am J Neuroradiol* 2009;30:917–22
- Bley T, Strother CM, Pulfer K, et al. C-arm CT measurement of cerebral blood volume in ischemic stroke: an experimental study in canines. *AJNR Am J Neuroradiol*. 2010;31:536–40
- Koenig M, Kraus M, Theek C, et al. Quantitative assessment of the ischemic brain by means of perfusion-related parameters derived from perfusion CT. *Stroke* 2001;32:431–37
- von Kummer R, Bourquain H, Bastianello S, et al. Early prediction of irreversible brain damage after ischemic stroke by computed tomography. *Radiology* 2001;219:95–100
- Synek V, Reuben JR, Du Boulay GH. Comparing Evans’ index and computerized axial tomography in assessing relationship of ventricular size to brain size. *Neurology* 1976;26:231–33
- Nguyen-Huynh MN, Wintermark M, English J, et al. How accurate is CT angiography in evaluating intracranial atherosclerotic disease? *Stroke* 2008;39:1184–88
- Bland JM, Altman DG. Statistical methods for assessing agreement between two methods of clinical measurement. *Lancet* 1986;1:307–10
- Muir KW, Buchan A, vonKummer R, et al. Imaging of acute stroke. *Lancet Neurol* 2006;5:755–68
- Parsons MW, Pepper EM, Bateman GA, et al. Identification of the penumbra and infarct core on hyperacute noncontrast and perfusion CT. *Neurology* 2007;68:730–36
- Murphy BD, Fox AJ, Lee DH, et al. White matter thresholds for ischemic penumbra and infarct core in patients with acute stroke: CT perfusion study. *Radiology* 2008;247:818–25
- Ahmed AS, Deuerling-Zheng Y, Strother CM, et al. Impact of intra-arterial injection parameters on arterial, capillary, and venous time-concentration curves in a canine model. *AJNR Am J Neuroradiol* 2009;30:1337–41
- Nogueira RG, Lev MH, Roccatagliata L, et al. Intra-arterial nicardipine infusion improves CT perfusion-measured cerebral blood flow in patients with subarachnoid hemorrhage-induced vasospasm. *AJNR Am J Neuroradiol* 2009;30:160–64. Epub 2008 Oct 22
- Covarrubias DJ, Rosen BR, Lev MH. Dynamic magnetic resonance perfusion imaging of brain tumors. *Oncologist* 2004;9:528–37